Supporting Information

Anion-exchange synthesis of an $MnCo_2S_4$ electrocatalyst towards facilitated ultralong hydrogen evolution reaction in acidic and alkaline Media

Abu Talha Aqueel Ahmed [a], Sankar Sekar [a,b], Shubhangi S. Khadtare [c], Nurul Taufiqu Rochman [d], Chinna Bathula [e], Abu Saad Ansari [d*]

[a] *Division of Physics and Semiconductor Science, Dongguk University, Seoul 04620, South Korea*

[b] *Quantum-functional Semiconductor Research Center, Dongguk University-Seoul, Seoul 04620, Republic of Korea*

[c] *Innovative Compound Semiconductor and Application Laboratory, Department of Electronic and Computer Engineering, Hanyang University, Seoul 04763, Republic of Korea*

[d] *Nano Center Indonesia Research Institute, Puspiptek street, South Tangerang, Banten 15314, Indonesia*

[e] *Division of Electronics and Electrical Engineering, Dongguk University, Seoul 04620, South Korea*

Corresponding Author: abusaadphy@gmail.com

Contents:

Table S1. Comparative electrochemical HER performance of various transition metal-based catalysts and the proposed $MnCo_2S_4$ catalysts in an acidic 0.5 M H_2SO_4 and alkaline 1.0 M KOH medium.

Obs. No.	HER catalysts	Electrolyte	Overpotential (η; mV) at –10 mA cm^{-2}	Tafel Slope (mV dec^{-1})	Ref.
1	Co:FeS_2/CoS_2@20 °C	0.5 M H_2SO_4	–90	66	S1
2	Mn-N-Co_9S_8	1 M KOH	–102	107.2	S2
3	FeO@CCS	1 M KOH	–107	136	25
4	N-CoS_2	0.5 M H_2SO_4	–97	101	26
		1 M KOH	–137	117	
5	Ce-$MnCo_2O_4$-3%	1 M KOH	–389	96	S3
6	$MnCo_2S_4$	1 M KOH	–167	136.74	30
7	MCO@NiFe LDH	1 M KOH	–129	112.5	21
9	(AgCuZnMnCoInGa)S	0.5 M H_2SO_4	–255	131.6	S4
9	Pt/NiS@Al_2O_3	0.5 M H_2SO_4	–34	~ 35	S5
10	Pt/NiS@Al_2O_3	0.5 M H_2SO_4	–34	~ 35	S6
11	$MnCo_2O_4$ nanosheets	0.5 M H_2SO_4	–138	119	**Present Work**
		1 M KOH	–149	128	
12	$MnCo_2S_4$ nanosheets	0.5 M H_2SO_4	–111	55	
		1 M KOH	–124	63	

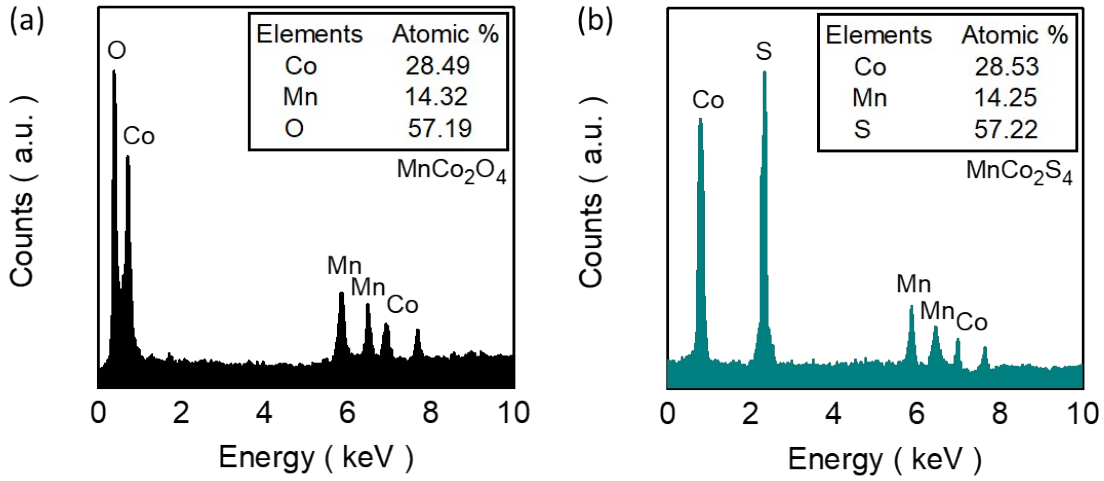

Fig. S1. EDS spectra for (a) $MnCo_2O_4$ and (b) $MnCo_2S_4$ electrodes, which confirms the complete transformation of oxide phase into sulfide form.

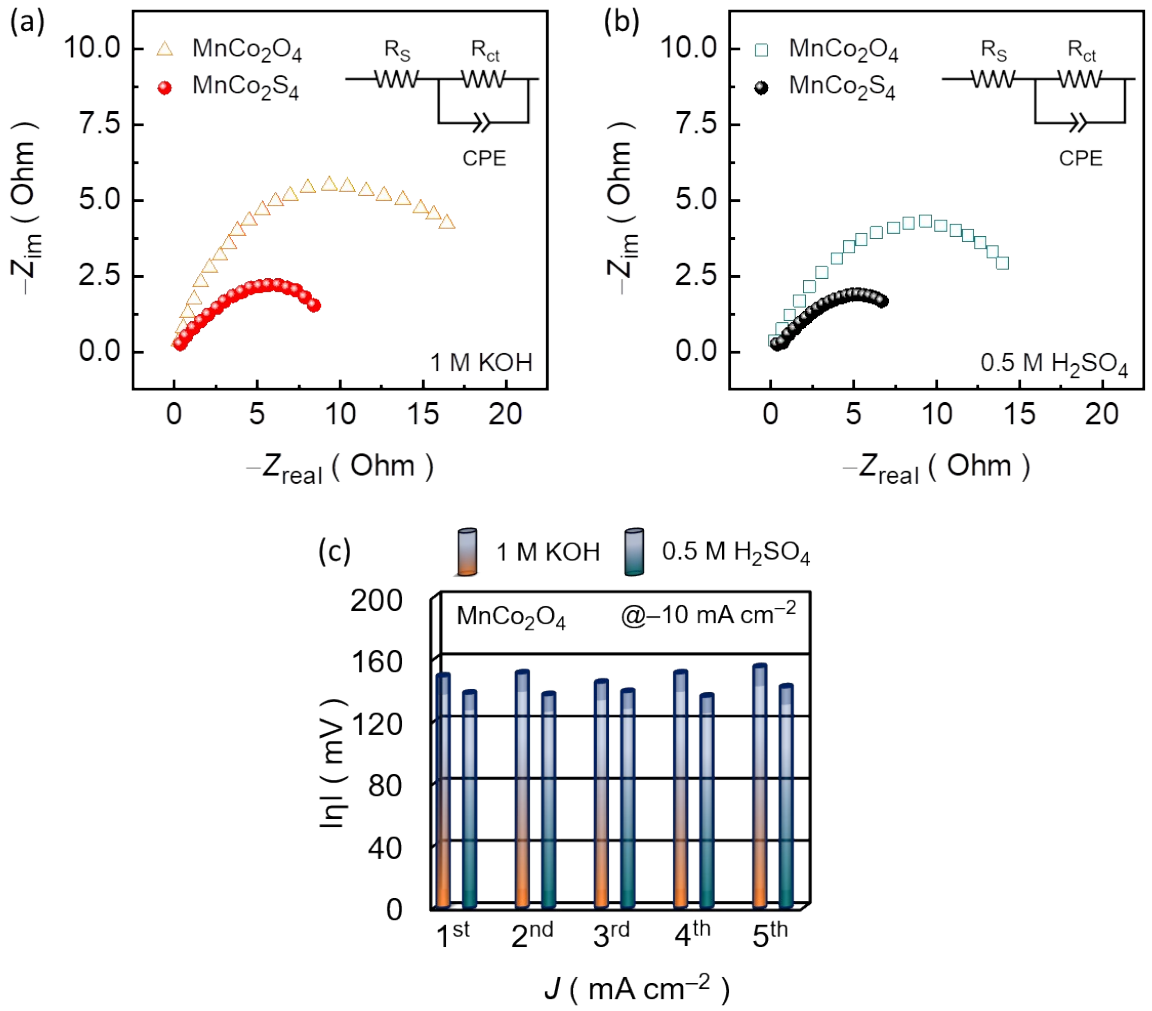

Fig. S2. EIS plots measured before and after stability in (a) alkaline 1 M KOH and (b) acidic 0.5 M H_2SO_4 medium. (c) Reliability graph for $MnCo_2O_4$ catalyst performance in acidic and alkaline media.

Table S2. EIS fitted parameters for $MnCo_2O_4$ and $MnCo_2S_4$ catalysts measured before and after stability.

$MnCo_2S_4$	**Before stability**		**After HER stability**	
	***R_S* (Ω)**	***R_{ct}* (Ω)**	***R_S* (Ω)**	***R_{ct}* (Ω)**
1 M KOH	0.368	8.488	0.394	9.113
0.5 M H_2SO_4	0.358	6.811	0.379	7.345

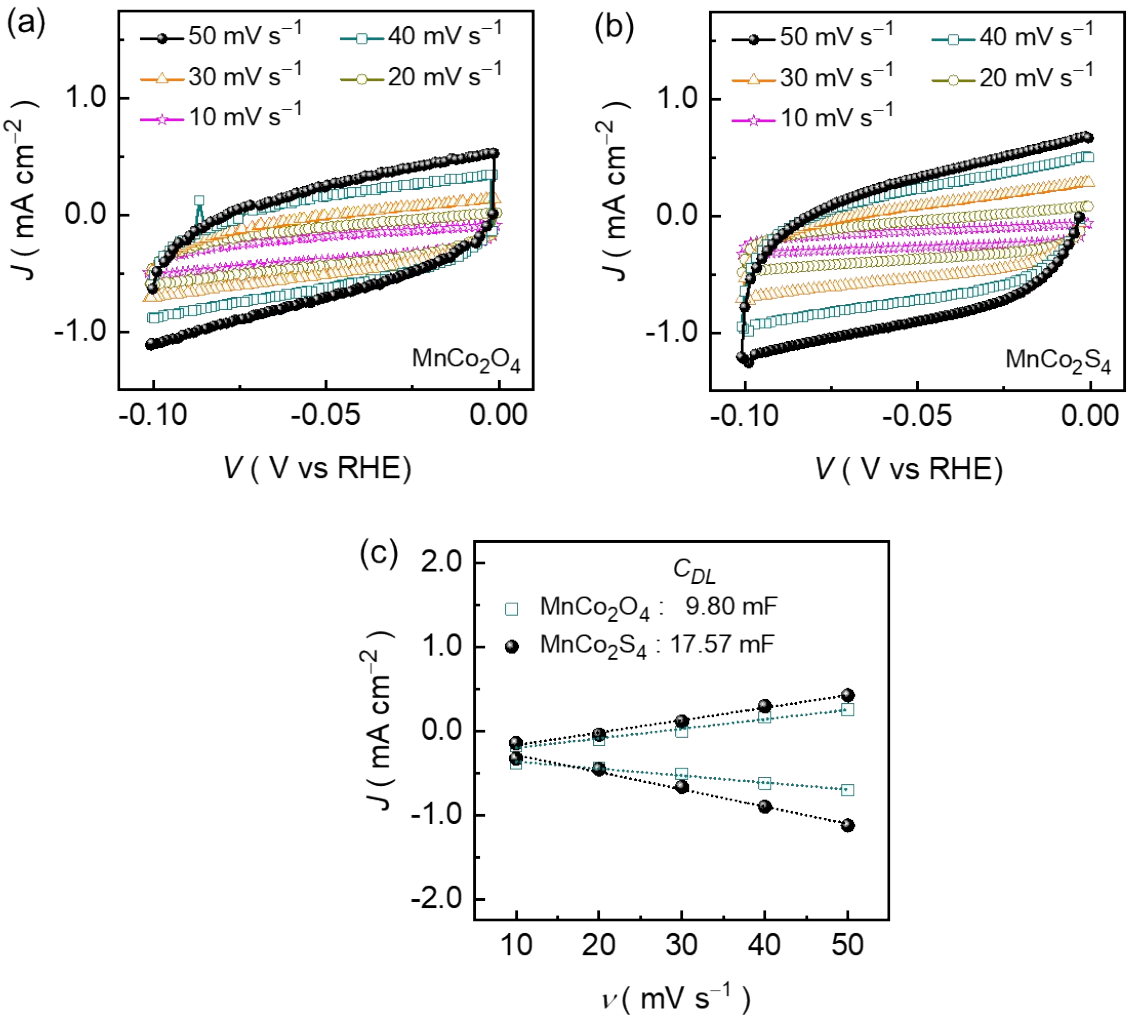

Fig. S3. Non-Faradaic scan rate-dependent CV curves for (a) $MnCo_2O_4$ and (b) $MnCo_2S_4$ catalysts recorded in a voltage window range between −0.10 and 0.00 V (*vs*. RHE). (c) "*J vs. v*" plot of $MnCo_2O_4$ and $MnCo_2S_4$ catalysts for the estimation of C_{DL} and *ECSA*.

Table S3. Estimated C_{DL} and *ECSA* values for $MnCo_2O_4$ and $MnCo_2S_4$ catalysts in alkaline KOH medium.

Catalysts	**C_{DL} (mF)**	**ECSA (cm^2)**
$MnCo_2O_4$	9.80	245
$MnCo_2S_4$	17.57	~ 439

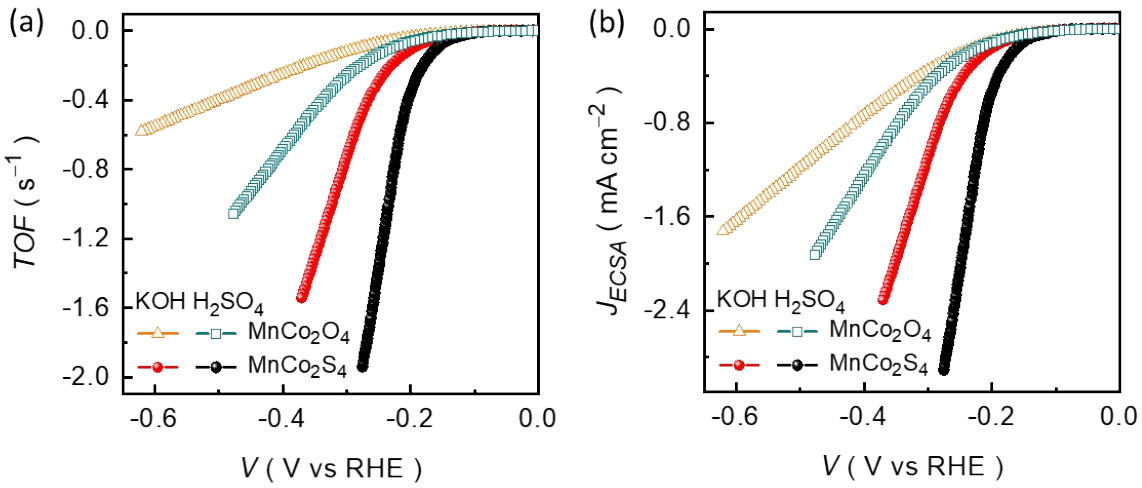

Fig. S4. (a) "*V vs. TOF*" plots and (b) *ECSA*-corrected LSV curves for $MnCo_2O_4$ and $MnCo_2S_4$ catalysts measured at 1.0 mV s^{-1} in an acidic (0.5 M H_2SO_4) and alkaline (1 M KOH) media.

The intrinsic reaction kinetics of the catalyst can be assessed by estimating the TOF values. Fig. S4a shows the "*V vs. TOF*" plots for the $MnCo_2O_4$ and $MnCo_2S_4$ catalysts calculated from the following equation as:

$$TOF = (J \times A) / (F \times n \times N) \quad \text{(S1)}$$

where *J*, *A*, *n*, *N*, and *F* signifies the current density, active catalyst loading area (1×1 cm^2), Faraday constant (96,485.3329 A s mol^{-1}), the number of moles of catalyst, and number of electrons mol^{-1} (for HER; N = 2), respectively. The $MnCo_2O_4$ catalyst demonstrates the *TOF* of –1.9393 and –0.4658 s^{-1} at –0.275 V in acidic and alkaline electrolyte media, respectively, which is comparatively lower than the $MnCo_2S_4$ catalysts (–0.1964 and –0.0980 s^{-1}) at the same potential value. The TOF for $MnCo_2S_4$ is almost 10- and 4-fold compared to pristine $MnCo_2O_4$ nanosheet catalyst in acidic and alkaline media, indicating that the after anion-exchange the intrinsic reaction kinetics improved significantly, which results in the efficient transportation of electron/ion throughout the 2D nanosheets. Moreover, *ECSA*-corrected

(J_{ECSA}) LSV curves further highlights the HER reaction kinetics, as shown in Fig. S4b catalysts. The J_{ECSA} plots reveals that the $MnCo_2S_4$ catalyst exhibits the smaller voltage response at each J_{ECSA} compared to the pristine $MnCo_2O_4$ catalyst, suggesting that $MnCo_2S_4$ catalyst has better intrinsic reaction kinetics.

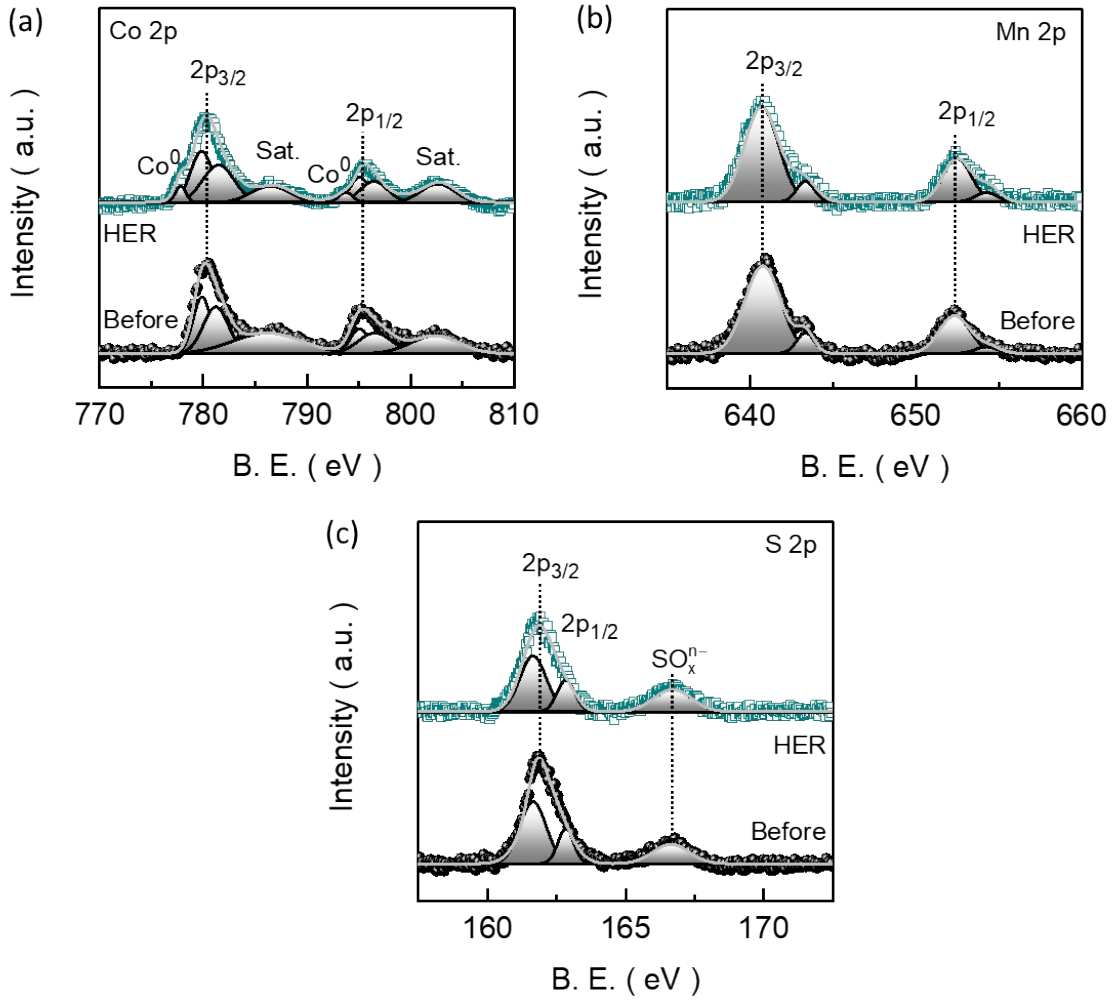

Fig. S5. Post-stability measured (a) Co 2p, (b) Mn 2p, and (c) S 2p high-resolution XPS emission spectra of $MnCo_2S_4$ catalyst.

Supporting References

S1. K. Wang, H. Song, Z. Lin, Y. Gao, H. Wu, S. Yan, J. Wang and Y. Shi, *Materials Express*, 2019, **9**, 786-791.

S2. Y. Xing, D. Li, L. Li, H. Tong, D. Jiang and W. Shi, *International Journal of Hydrogen Energy*, 2021, **46**, 7989-8001.

S3. X. Huang, H. Zheng, G. Lu, P. Wang, L. Xing, J. Wang and G. Wang, *ACS Sustainable Chemistry & Engineering*, 2019, **7**, 1169-1177.

S4. W. Xiao, Y. Li, A. Elgendy, E. C. Duran, M. A. Buckingham, B. F. Spencer, B. Han, F. Alam, X. Zhong, S. H. Cartmell, R. J. Cernik, A. S. Eggeman, R. A. W. Dryfe and D. J. Lewis, *Chemistry of Materials*, 2023, **35**, 7904-7914.

S5. Y. Feng, Y. Guan, H. Zhang, Z. Huang, J. Li, Z. Jiang, X. Gu and Y. Wang, *Journal of Materials Chemistry A*, 2018, **6**, 11783-11789.

S6. G. Ghanashyam and H. Kyung Jeong, *Inorganica Chimica Acta*, 2022, **541**, 121098.